IOP Publishing Plasma Sources Science and Technology
Plasma Sources Sci. Technol. **28** (2019) 095010 (11pp) https://doi.org/10.1088/1361-6595/ab3c2f

Tuning the composition of plasma-activated water by a surface-wave microwave discharge and a kHz plasma jet

Kinga Kutasi[1], Dean Popović[2], Nikša Krstulović[2] and Slobodan Milošević[2]

[1] Wigner Research Centre for Physics, Institute for Solid State Physics and Optics, Hungarian Academy of Sciences, POB 49, H-1525 Budapest, Hungary
[2] Institute of Physics, Bijenička cesta 46, 10000 Zagreb, Croatia

E-mail: kutasi.kinga@wigner.mta.hu

Received 8 March 2019, revised 25 June 2019
Accepted for publication 16 August 2019
Published 6 September 2019

Abstract

An atmospheric pressure surface-wave microwave discharge and a kHz plasma jet are used to activate purified water. It is shown, that by varying the treatment distance and the initial $Ar/N_2/O_2$ mixture composition of the surface-wave microwave discharge the concentration ratio of NO_3^- and H_2O_2 radicals created in the plasma activated water (PAW) can be varied over three orders of magnitude, which can be preserved during months of storage at room temperature. At the same time, with the 5 min treatment of the 32 ml water the absolute radical concentrations are varied in the range of 0.5–85 mg l^{-1} for H_2O_2, 20–180 mg l^{-1} for NO_3^- and 0.5–14 mg l^{-1} for NO_2^-. In the case of the N_2 kHz plasma jet this concentration ratio can be tuned within one order of magnitude by varying the treatment distance. By treating different volumes very similar concentration ratios are obtained, which evolve differently during storage, as the ageing dynamics is determined by the absolute concentration of radicals. In general, the radical most affected by ageing is NO_2^-, whose recombination is found to be determined by the H_2O_2 radical. In order to control the H_2O_2 concentration and thus the NO_2^- radicals recombination, the application of a Fenton type reaction is suggested, which is implied by inserting a copper surface into PAW during or after plasma treatment.

Keywords: plasma activated liquids, surface-wave microwave discharge, plasma jet

1. Introduction

In the last decade plasma-activated water (PAW), or more generally plasma-activated liquid (PAL) has received a lot of attention from the plasma medicine and plasma agriculture community due to its potential to induce oxidative stress to cells. By PAL it is meant the liquid which contains reactive species, mostly reactive oxygen and nitrogen species (RONS), generated by the interaction of active or afterglow plasma with the liquid. PAW has been found to have antimicrobial and antibacterial effect [1–9], which is thought to occur due to the synergetic effect between the RONS and/or pH of the solution [3, 5]. Plasma activated buffered solution and cell culture media has also been studied for therapeutical aims [10–12], and it has been shown its potentials for cancer therapy [11]. In the field of agriculture with PAW the improvement of seeds germination and plant growth have been targeted [13–15].

The lifetime of PAL has been found to be very different, varying from days to months, depending on the plasma source used. Several works define the PAL lifetime as its activity retention time [16–19], while others follow the lifetime of different RONS in the PAW [5, 16, 18–20]. The main long-lived RONS produced in PAL have been identified to be the H_2O_2, NO_3^- and NO_2^- [21]. In a 60 ml ns pulsed DBD air plasma treated water the NO_2^- molecules could be detected up to 25 min, while the concentration of H_2O_2 decreased by a factor of 2 [18]. On the other hand in a 10 ml DBD activated water Traylor *et al* [5] have found that the lifetimes of H_2O_2 and nitrite are up to 4 d, while the nitrate concentration

Table 1. Typical plasma activated liquids found in the literature. Concentration of long lived radicals in PALs created with different plasma sources in deionized water (DIW), phosphate buffer saline solution (PBS), phosphate buffer (PB) and 5 mmol l^{-1} *N*-acetyl-cysteine in PBS (NAC), respectively.

Liquid	Plasma system	V [ml]	t [min]	pH	$[H_2O_2]$ [mg l^{-1}]	$[NO_2^-]$ [mg l^{-1}]	$[NO_3^-]$ [mg l^{-1}]	References
DIW	Air gliding arc	20	5	3.0	0.34	73	8	[3]
DIW	Air DBD	10	30	2.7	3	1.0	64	[6]
DIW	Air DBD	5	30	2.7	18	1.5	113	[6]
DIW	Air DC microjet	20	20	3.2	80	21	37	[32]
DIW	He rf jet	0.5	5	4.2	50	—	—	[4]
DIW	Air DBD	10	20	2.7	3.4	55	74	[5]
DIW	Air corona	10	60	2.8	50	—	—	[16]
PBS	Air corona	10	60	6.5	100	—	—	[16]
Water	Negative corona	—	180	—	3	120	—	[30]
PBS	Air DBD	0.15	5	6.5	2.7	161	186	[33]
NAC	Air DBD	1	3	2.58	30	—	239	[34]
Saline	Ar rf jet	3.35	33	4.1	20	0.5	6	[35]
Water	Electrospray spark	2.5	5	3.3	24	9	62	[25]
PB	Electrospray spark	2.5	5	6.2	14	28	56	[25]
PB	Pulsed DC	900	30	3.3	7	4	8	[21]
DIW	Air ns DBD	60	5	2.7	8.5	7	93	[18]
DIW	Air ns DBD	60	10	2.3	10	4.6	217	[18]
PBS	He-1%N_2 DBD jet	2	10	7.2	—	27	28	[36]
DIW	Air rf microjet	35	30	2.1	10	0	155	[37]
DIW	He rf microjet	35	30	2.3	15	0	93	[37]
DIW	Ar rf microjet	35	30	2.6	24	0	93	[37]
DIW	He DC jet	0.3	2	—	27	—	—	[38]
DIW	He BDB jet	3	30	—	3.43	1.69	0.79	[39]

increases slightly during the 7 d of observation. Julák *et al* [16] have observed the total disappearance of H_2O_2 (initial concentration of about 5 mg l^{-1}) from the 10 ml corona discharge treated water in 1 month. Shen *et al* [19] have followed the evolution of species concentration—0.81 mg l^{-1} of H_2O_2, 1.2 mg l^{-1} of NO_2^- and 14.6 mg l^{-1} of NO_3^- –in 10 ml microjet activated water stored at different temperatures: 25 °C, 4 °C, −20 °C and −80 °C. At 25 °C after 30 d the initial concentration of H_2O_2 decreased by a factor of 5, of NO_2^- by a factor of 8, while that of NO_3^- by a factor of 3. By lowering the storage temperature the recombination of H_2O_2 and NO_2^- decreased, and the freezing of NO_2^- could be realized at −80 °C. Julák *et al* [20] have stored the 30 min air corona treated 1.5 ml water at 4 °C over 1 year and have measured the decrease of the initial 126 mg l^{-1} H_2O_2 to 41 mg l^{-1}.

Lukes *et al* [21] have shown that the concentration of species and their lifetime depend on the pH of treated water. At acidic conditions (pH 3.3) lower concentrations of NO_2^- and H_2O_2, and higher concentrations of NO_3^- were detected as compared to conditions of pH 6.9 and 10.1. At the same time during the after-treatment period under acidic conditions the NO_2^- and H_2O_2 concentrations decreased, and that of NO_3^- increased, while at higher pHs the concentrations did not change.

The typical concentrations reported in the literature for the main RONS are summarized in table 1. Several studies have been triggered by the plasma medicine applications, therefore a small quantity of liquids have been treated, volumes of typical cell culture plates. Higher treated volumes range between 10 to 60 ml, and depending on the plasma source used very different species concentrations are obtained. However, these works report typically one or two PAL conditions, giving no further suggestions for PAL composition tuning. In order to be able to identify the role of different species and to clarify the synergy effects in the interaction of PAL with biological systems, PAL with different compositions would be welcomed, in what concerns the density ratios of different RONS. For tuning the PAW composition an attempt has been done by Ito *et al* [22] by using a He DBD jet with different shielding gases, thus obtaining ratios of $[NO_2^-]/[H_2O_2]$ ranging between 0 and 0.18. However, here no information is given about the density of NO_3^- molecules, which can be also formed during storage from the reaction of NO_2^- with H_2O_2 [21]. By transforming an air DBD into a DBD jet by flowing He through the array electrode, a slight tuning of the species concentration in the treated water has been achieved when varying the gas flow rate in the 0–8 slm range [23]. Namely, in an 8 ml 3 min treated DIW the H_2O_2 concentration increased from 0.3 to 5.8 mg l^{-1}, the concentration of NO_2^- decreased from 5.5 to 1.4 mg l^{-1} and that of NO_3^- varied between 19.8 and 13.6 mg l^{-1}, while the pH ranged between 2.4 and 2.7.

In the present work the tuning possibility of PAW composition through the treatment of purified water with a surface-wave microwave discharge and a kHz plasma jet is studied. Furthermore, the ageing of PAWs with different

compositions are also followed, and solutions for controlling the PAW ageing are searched for.

2. Plasma systems and production of plasma activated water

Active species have been generated in purified water by putting the water surface in contact with the plasma plume of a kHz plasma jet and a surface-wave microwave discharge, respectively. The water samples are analyzed immediately after the treatment, as well as several times during the three months of storage. The samples are kept in closed containers (clearglass container from Macherey-Nagel GmbH) filled up to few mm below cap, at room temperature (20 °C–22 °C) and predominantly in dark.

The concentration of NO_2^-, NO_3^- and H_2O_2, and the pH of samples are measured with QUANTOFIX® test strips (Nitrate/Nitrite 500: 10–500 mg l^{-1} NO_3^-, 0.5–80 mg l^{-1} NO_2^-; Nitrate/Nitrite 100: 5–100 mg l^{-1} NO_3^-, 0.5–50 mg l^{-1} NO_2^-; Peroxide 25: 0.5–25 mg l^{-1}; Peroxide 100: 0.5–25 mg l^{-1}) and evaluated with the QUANTOFIX® Relax unit (by Macherey-Nagel, GmbH). The test strips calibrated by the producer to certified standard solutions allow fast analyzing without the waste of the sample, thus making possible to follow the ageing of PAWs even with high temporal resolution. On the other hand, the QUANTOFIX Relax reader allows quantitative analysis of strips with high accuracy[3]. The measuring error has been determined to be less than 10% (typically 6%–8%).

2.1. Plasma jet

The atmospheric pressure plasma jet consists of a quartz tube with the outer and inner diameters of 1.5 and 1 mm, respectively, and a copper wire of 100 microns diameter, which is inserted in the capillary and serves as the powered electrode [24]. The powered electrode is connected to a high voltage power supply, which provides a sinusoidal waveform of 28 kHz with 12 kV maximum voltage. The discharge is ignited in N_2 gas (99.996% purity), which is supplied into the capillary typically with a flow rate of 500 sccm. The purified water—commercial purified water of Pharmaceutical degree (Pharmacopoeia Europaea, Ph. Eur. 9) with pH 6.5 from the KEMIG d.o.o. Croatian company—in Berzelius beaker is brought in contact with the plasma jet by placing the water surface from the capillary orifice at distances in the 1–10 mm range. The treated volumes have been 25, 125 and 200 ml.

2.2. Surface-wave microwave discharge

The surface-wave microwave discharge is generated with the help of a surfatron launcher (Sairem, Surfatron 80) in a quartz tube of outer diameter 6 mm and inner diameter 4 mm, using as a main gas Ar at gas flow rates of 1500–2000 sccm. During experiments Ar-N_2/O_2 binary and ternary mixtures are also used with the O_2 and N_2 gas flow rates ranging between 10 and 100 sccm. The input power is varied between 25 and 30 W, while the reflected power can be up to a maximum of 1 W. The quartz tube is fixed inside the surfatron in such a way, that downstream from the closing plate of the surfatron the edge of the quartz tube is at 14.5 mm distance. This insures that at the powers and gas flow rates used the plasma plume outside the tube is long enough to allow different contact points with the water surface. A Berzelius beaker of 35 ml filled with 32 ml of purified water is positioned below the plasma plume with the water surface being at 5.5, 8.5 or 10.5 mm distances from the edge of the quartz tube. The purified water is produced with the ELGA Purelab Option-R 7 purifier and is characterized by Total Organic Carbon (TOC) <20 ppb, Bacteria <1 CFU/ml, Inorganic-Typical >15 MΩcm. In order to avoid the overheating of the quartz tube during treatments, compressed air is applied along the quartz tube with a gas flow rate of 8 slm, which on the other hand has also shielding effect. The surface-wave microwave discharge being an electrodeless discharge can have a significant advantage by avoiding the contamination of liquid with nanoparticles originating from the sputtering of the electrodes, as observed in some cases [25]. Due to their advantages surface wave-microwave discharges have also been studied for biological applications [26].

The surface-wave microwave discharges have also the advantage of the high flexibility in tuning the plasma composition [27]. The surface-wave microwave discharge consists of a plasma column, characterized with a decreasing electron density profile along the column, with the critical electron density occurring at the end of it [28]. At atmospheric pressure the plasma column can extend over the discharge tube (with a slight change in the electron density profile at the exit of the quartz tube due to the change of the guiding dielectric [26]), as shown in figure 1. Due to this property, by changing the distance between the discharge tube and the water surface, different electron density can be achieved at the interaction surface. In our study, as a reference condition it is chosen the 2000 sccm Ar and 25 W discharge, with the discharge tube-water surface distance of 5.5 mm. In order to vary in the plasma plume the density of NO and NO_2 molecules (which contribute to the formation of nitrite and nitrate ions in the PAW), N_2 and O_2 gases can be added to Ar. The sustainment of the discharge and the length of the plasma column depend on the power absorption of electrons from the electromagnetic field, which is determined by the electron collision frequencies [29]. When molecular gasses are added to argon, due to the change of the power absorption, larger input power is necessary to sustain a stable discharge, while the length of the plasma column also decreases, as illustrated in figure 1. Therefore, using different $Ar/N_2/O_2$ mixtures and treatment distances, both the electron and the NO and NO_2 densities can be tuned at the plasma-water interaction surface.

[3] We have also performed test measurements on chemically prepared solution characterized as 0 mg l^{-1} H_2O_2, 2 mg l^{-1} NO_2^- and 50 mg l^{-1} NO_3^-. The strip measurements have been performed after freezing and defrosting the solution, and obtained concentrations of 0 mg l^{-1} H_2O_2, 2.1 mg l^{-1} NO_2^- and 55 mg l^{-1} NO_3^-.

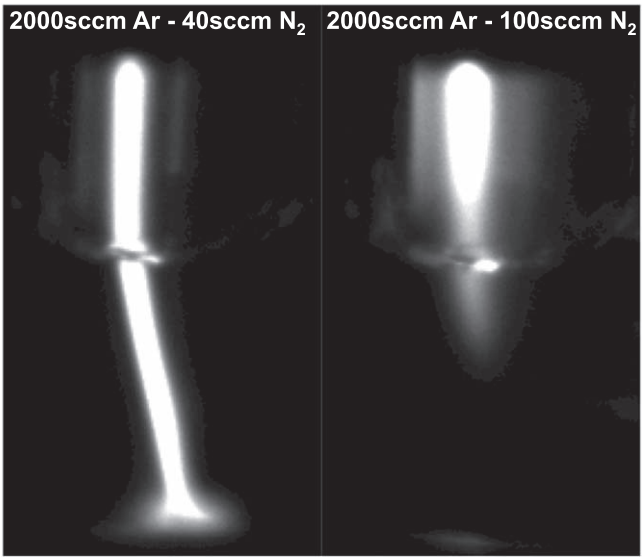

Figure 1. Image of the plasma plume in the case of 2000 sccm Ar—40 sccm N_2 27 W and 2000 sccm Ar—100 sccm N_2 30 W surface-wave microwave discharges.

3. Results and discussion

3.1. The PAW produced with the surface-wave microwave discharge

Table 2 shows the different treatment conditions applied and the characteristics of the generated plasma activated water. First of all, different Ar discharge conditions have been tested by changing the gas flow rate and the treatment distance. As the plasma plume is characterized by a decreasing electron density profile, by changing the treatment distance the electron density is also changed at the plume-water surface interaction point. The electrons interacting with water molecules at the gas–water interface can create OH radicals, which afterwards in the $OH + OH \longrightarrow H_2O_2$ recombination reaction form H_2O_2. This is well illustrated by the obtained results, namely, at the lower treatment distance, where higher electron density occurs at the water surface, higher H_2O_2 concentration is obtained (condition Ar_1 versus Ar_2). By decreasing the gas flow rate (the Ar_3 condition), the plasma plume becomes slightly shorter, while more air is able to diffuse into the plume, which favours the formation of nitrate and nitrite radicals.

Figure 2 shows the spectra of the plume close to the water surface in the case of two different quartz tube-water surface distances. The intensity of the OH band (the OH(A–X) transition (0, 0) bandhead at 308.5 nm) is considerably lower comparing to the N_2 bands and Ar lines intensity, suggesting, that the OH radicals are created at the gas–liquid interphase, instead of the plasma plume. The spectra show, that the emission of the Ar states excited by electrons (in the 602–760 nm spectral range) are lower at the higher treatment distance, indicating a lower electron density. Additionally, we can also observe the emission of the NOγ and NOβ bands (200–300 nm range)—which is a good indication for the presence of NO molecules—with higher intensity at the higher treatment distance. Meanwhile at the lower treatment distance, there is a marked signal of the NO_2 green–yellow continuum, showing the presence of NO_2 molecules. The dissolved NO and NO_2 molecules contribute to the creation of nitrate and nitrite radicals in PAW through the following reactions:

$$NO_{2(aq)} + NO_{2(aq)} + H_2O_l \longrightarrow NO_2^- + NO_3^- + 2H^+, \quad (1)$$

$$NO_{(aq)} + NO_{2(aq)} + H_2O_l \longrightarrow 2NO_2^- + 2H^+, \quad (2)$$

$$NO_{(aq)} + OH_{(aq)} \longrightarrow NO_2^- + H^+, \quad (3)$$

$$NO_{2(aq)} + OH_{(aq)} \longrightarrow NO_3^- + H^+. \quad (4)$$

Additionally, the formation of NO_3^- is also promoted through the $NO_2^- + H_2O_2 + H^+ \longrightarrow NO_3^- + H_2O + H^+$ reaction, which results in relatively lower NO_2^- concentration comparing to NO_3^-.

By adding N_2 to Ar (conditions Ar_N_2 in table 2) the length of the plasma plume decreases, while the plasma becomes stable only at a higher 27 W power. This effect is well reflected by the lower H_2O_2 concentrations obtained with the Ar-N_2 discharges comparing to Ar discharges (see Ar_1 versus ArN_2_1 condition). Figure 3 shows the spectra close to the water surface when adding 40 sccm, 60 sccm and 100 sccm N_2, respectively, to Ar in the case of 5.5 mm treatment distance. Comparing to the spectra of the Ar discharge (figure 2) the intensity of Ar lines gradually decreases with the N_2 addition, which also indicates the lowering of the electron density. With the addition of 100 sccm of N_2 the emission intensity decreases significantly, which indicates, that the plasma plume becomes so short, that the water surface interacts with the plasma afterglow, as also illustrated by the plasma plume images in figure 1. Along the afterglow the electron density drops fast, while the density of NO and NO_2 radicals also decrease. This results, as expected, in a lower H_2O_2 and nitrite/nitrate concentrations.

The NOγ emission is also well observed in the afterglow region due to the fact that here the excited NO(A) molecules are created mostly through the three body recombination of N and O atoms. The afterglow conditions are also approached when increasing the treatment distance in the case of 40 sccm and 60 sccm N_2 mixture discharges, resulting in lower species concentrations in the PAW: ArN_2_1 versus ArN_2_3 conditions, and ArN_2_5 versus ArN_2_6, respectively. ArN_2_6 and ArN_2_7 conditions show, that similar effect can be obtained by decreasing the gas flow rate instead of changing the treatment distance. It is also found, that the doubling of the treatment time (ArN_2_3. versus ArN_2_4. condition) practically doubles the active species concentrations in PAW.

When adding O_2 to the Ar-N_2 mixture, the discharge can be sustained at a lower power of 25 W, similar to the case of pure Ar. Due to the lower input power and the different power absorption along the plasma column, the electron density along the plasma plume is lower than in the case of the 27 W input power Ar-N_2 mixture, which is well reflected by the lower H_2O_2 concentration obtained in the PAW: ArN_2O_2_1 versus ArN_2_1 in table 2. On the other hand, when O_2 is added to the pure Ar, such in the case of 20 sccm O_2 to 2000 sccm Ar (ArO_2_1), the discharge's structure is very

Table 2. The treatment conditions: gas flow rates, input power and quartz tube-water surface distance, and the surface-wave microwave discharge produced PAW's characteristics at different ageing moments. The PAWs could be reproduced with a maximum error of 5%.

I.D.	Conditions	t [min]	$[H_2O_2]$ [mg l^{-1}]	$[NO_2^-]$ [mg l^{-1}]	$[NO_3^-]$ [mg l^{-1}]	[pH]
Ar_1.	2000 sccm Ar	0	84	6.8	92	5.7
	25 W, 5.5 mm	95	63	0.5	49	4.6
		83 567	50	0.5	40	6.6
Ar_2.	2000 sccm Ar	0	60	16	178	5.8
	25 W, 10.5 mm	90	28	0.5	55	4.4
Ar_3.	1500 sccm Ar	0	46	12	123	5.4
	25 W, 5.5 mm	93	25	1.6	61	5.1
		83 554	21	0.5	55	6.2
ArN_2_1.	2000 sccm Ar-40 sccm N_2	0	40	12	136	5.3
	27 W, 5.5 mm	82	36	1.3	63	4.3
		83 535	23	0.5	56	6.3
ArN_2_2.	1500 sccm Ar-40 sccm N_2	0	9	9.6	104	5.6
	27 W, 5.5 mm	86	9	5.6	80	5.5
		83 540	2.4	0.5	40	6.6
ArN_2_3.	2000 sccm Ar-40 sccm N_2	0	2	6.6	73	5.8
	27 W, 10.5 mm	81	2	5.9	79	5.4
		83 529	0.5	1.6	36	6.5
ArN_2_4.	2000 sccm Ar-40 sccm N_2	0	4	14	141	5
	27 W, 10.5 mm, 10 min	92	3	6.3	101	5.3
		83 488	0.5	0.5	61	5.8
ArN_2_5.	2000 sccm Ar-60 sccm N_2	0	17	8.7	128	5.5
	27 W, 5.5 mm	68	25	2.8	68	4.8
		83 508	15	0.5	51	6.3
ArN_2_6.	2000 sccm Ar-60 sccm N_2	0	3	4.9	62	5.8
	27 W, 8.5 mm	79	4	4	55	5.8
		83 520	0.5	0.5	24	6.6
ArN_2_7.	1500 sccm Ar-60 sccm N_2	0	3	4.5	59	6
	27 W, 5.5 mm	66	3	3.4	52	6
		83 503	0.5	0.5	22	6.7
ArN_2_8.	2000 sccm Ar-100 sccm N_2	0	11	6.5	73	5.8
	30 W, 5.5 mm	84	11	3.8	52	5.5
		83 484	5	0.5	29	6.4
ArN_2O_2_1.	2000 sccm Ar-40 sccm N_2-10 sccm O_2	0	20	8.8	104	5.4
	25 W, 5.5 mm	76	19	1.8	59	5.5
		83 486	16.6	0.5	53	5.8
ArN_2O_2_2.	2000 sccm Ar-40 sccm N_2-20 sccm O_2	0	37	12	128	5.3
	25 W, 5.5 mm	74	14	2.7	64	4.9
		83 484	8.5	0.5	43	5.9
ArO_2_1.	2000 sccm Ar-20 sccm O_2	0	80	9.3	113	5.5
	25 W, 5.5 mm	73	37	0.5	50	4.9
		83 451	43	0.5	45	5.8
ArO_2_2.	2000 sccm Ar-40 sccm O_2	0	75	13	122	5
	27 W, 5.5 mm	84	41	1	66	4.4
		83 388	35	0.5	57	5.9

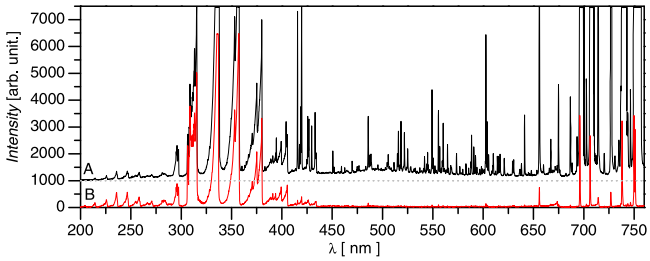

Figure 2. Spectra of plasma plume close to the water surface for different quartz tube-water distances: (A) $d = 5.5$ mm and (B) $d = 10.5$ mm, in the case of the 2000 sccm Ar, 25 W discharge. The spectra are shifted in intensity for clarity.

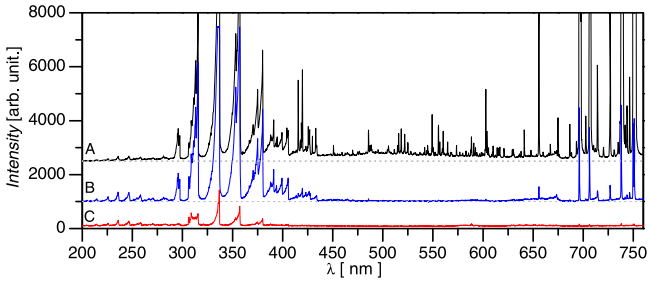

Figure 3. Spectra of plasma plume close to the water surface for (A) 2000 sccm Ar—40 sccm N_2 27 W, (B) 2000 sccm Ar—60 sccm N_2 27 W and (C) 2000 sccm Ar—100 sccm N_2 30 W. The spectra are shifted in intensity for clarity.

similar to that of the pure Ar discharge (Ar_1), which is also shown by the obtained similar H_2O_2 concentrations (and the measured spectra, not shown here, where the emission intensity of Ar I lines were found to be similar as in the case of Ar discharge), while in the case of the Ar-O_2 mixture higher nitrate/nitrite concentrations are obtained, due to the higher creation probability of the NO_2 radicals in the gas phase. With the increase of the O_2 gas flow rate in the Ar-O_2 mixture (ArO_2_2) the density of NO_2 radicals can be further increased, resulting in higher nitrate and nitrite production in PAW.

The ageing of the PAW at room temperature, already shown by the data presented in table 2, is further illustrated in figure 4 at conditions with very different initial hydrogen peroxide levels in the PAW. The figures indicate that the ageing dynamics depends on the H_2O_2 concentration, and in each case the concentrations stabilize after one week.

The most sensitive radical is found to be the NO_2^-, also due to its low concentration. In the case of initially high H_2O_2 concentrations the NO_2^- radicals recombine within the first hour, while at considerably lower H_2O_2 concentrations, figure 4(d) and (f), the recombination of NO_2^- slows down. At very low initial H_2O_2 concentrations the NO_2^- can survive more than one month. This indicates, that the main recombination pathway for NO_2^- could be the $NO_2^- + H_2O_2 + H^+ \rightarrow NO_3^- + H_2O + H^+$ process. This reaction is found to be effective in acidic conditions (pH < 6) [30], a constant rate being reported for conditions with pH between 4 and 6 at 25 °C [31]. In the case of H_2O_2 and NO_3^- radicals we can observe a sharp decrease of concentrations within the first hour, when both initial concentrations are higher than about 60 mg l^{-1}, figures 4(a) and (b). At lower initial H_2O_2 concentrations (10–40 mg l^{-1}), figures 4(c) and (d), the recombination rates for both radicals become smaller, more pronouncedly in the case of H_2O_2. Furthermore, when the initial H_2O_2 concentration is lower than 5 mg l^{-1} the H_2O_2 radicals disappear totally within one week.

Another important characteristics of PAW is the pH, which is also shown in table 2, as well as its post-discharge evolution. Comparing the different PAWs at $t = 0$ min, as expected based on the reactions (1)–(4), the pH correlates with the nitrite/nitrate concentrations, namely, at higher nitrate concentration lower pH is obtained. However, during the first hour of ageing, when a sharp decrease of concentrations occurs, the pH also decreases, except for the conditions where the H_2O_2 concentration is initially very low e.g. ArN_2_4 and ArN_2_6 conditions. This suggests the influence of the first phase H_2O_2 recombination on the pH, i.e. on the H^+ ion concentration. In order to understand the complex dynamics of the system, a detailed investigation of the processes is needed, which will be the focus of a next work.

Figure 5 (a) and (b) summarizes the different PAW compositions obtained with the treatments listed in table 2 right after the treatment and after one hour of storage, respectively. As already shown in figure 4, during the first hour both the nitrate and hydrogen peroxide concentrations decrease, resulting in a considerable change of the PAW's composition. Figure 5 illustrates the possible PAWs to be obtained with a surface-wave microwave discharge. We note, that with doubling the treatment time, the doubling of the concentrations has been achieved (ArN_2_3 versus ArN_2_4). Comparing to the condition with the largest H_2O_2 in figure 5(a) (84 mg l^{-1} H_2O_2 and 92 mg l^{-1} NO_3^-), higher H_2O_2 concentration and corresponding lower NO_3^- concentration can be achieved by further decreasing the treatment distance or increasing the input power in the case of the Ar discharge. For the given condition, the corresponding NO_3^- concentration can be further decreased by increasing the Ar gas flow rate, which results in lower air inflow into the plasma plume from the surroundings. On the other extreme, at very low H_2O_2 concentrations, the treatments occur close to the afterglow conditions. By further increasing the treatment distance (or decreasing the input power), only neutral species would interact with the water surface, which results in H_2O_2 free PAWs. The nitrite-hydrogen peroxide concentration map, figure 5(b), shows the limit for the H_2O_2 content of PAW where NO_2^- radicals can survive longer than one hour, namely in the case of H_2O_2 concentrations below 30 mg l^{-1}.

Finally, figure 6 shows the ratio of the nitrate to hydrogen peroxide concentration as a function of ageing for the different treatment conditions as listed in table 2. By changing the treatment distance and the initial gas mixture composition of the discharge, the $[NO_3^-]/[H_2O_2]$ concentration ratio can be varied over three orders of magnitude from about 0.5 to 150 (we note that the lowest detection limit of H_2O_2 is 0.5 mg l^{-1}, thus in the ratio calculations the concentrations that are lower than that value are taken as 0.5). In the case of

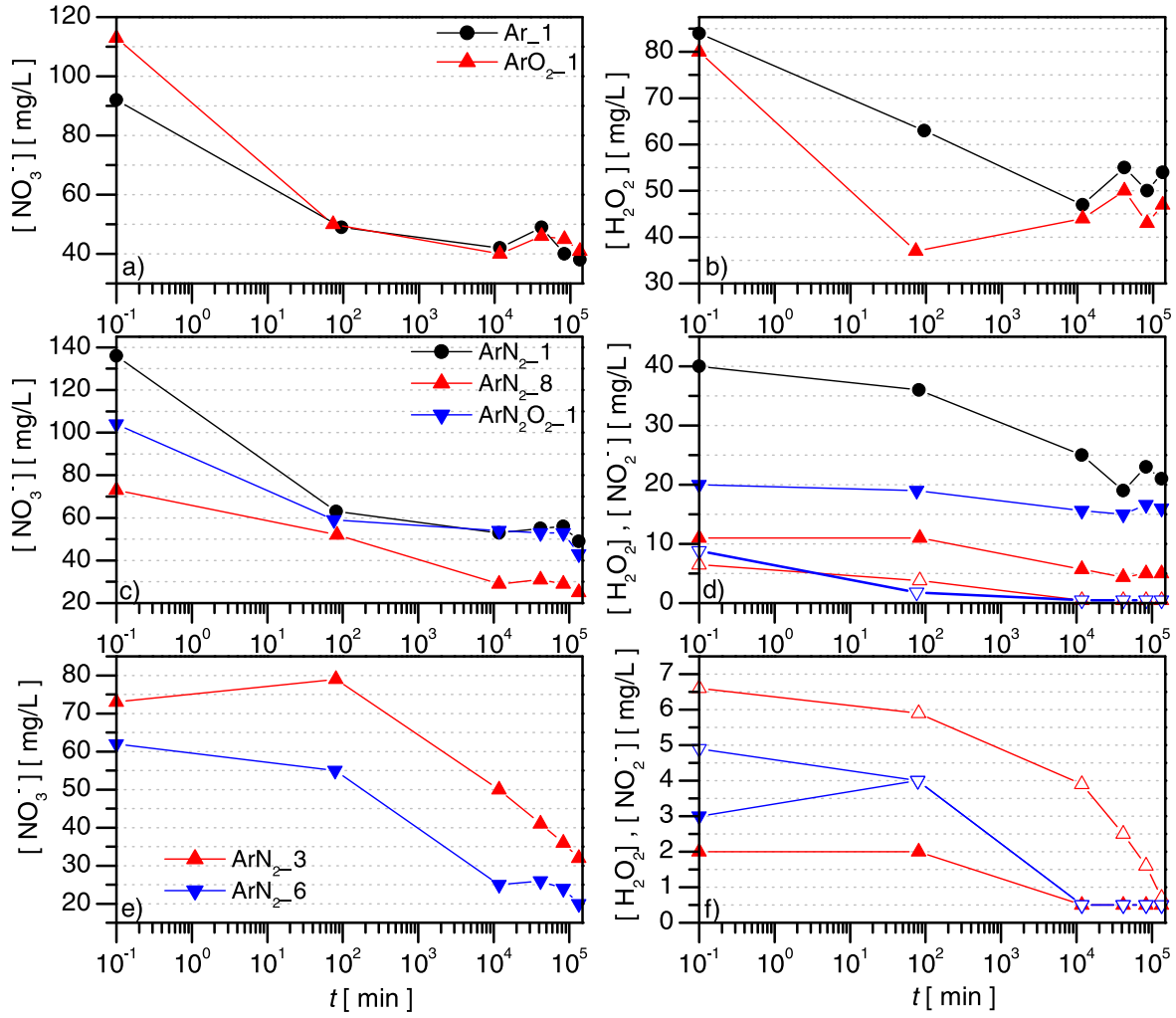

Figure 4. Evolution of radical concentration during PAW storage at room temperature for different treatment conditions. In the right column for the same conditions the closed symbols represent the concentration of H_2O_2, while the open symbols that of NO_2^-.

the treatment conditions where initially ($t = 10$ s) low H_2O_2 concentrations are obtained, the ageing has a more pronounced effect on the concentrations ratio, due to the strong recombination of H_2O_2, while the NO_3^- recombination is much slower (see figures 4(e)–(f)).

3.2. The PAW produced with the kHz plasma jet

Comparing to the surface-wave microwave discharge, the kHz plasma jet can be more easily ignited in molecular gases, such as nitrogen and oxygen, and consequently in air. For large scale applications, from the economical point of view, this system could have the advantage of using air or air like mixtures instead of more costly rare gases. Figure 7 shows the optical emission spectra of a nitrogen and an argon kHz plasma jet. In both cases the nitrogen band exhibit similar intensities, while in argon discharge a strong OH band (309 nm) emission also appears. This could be related to the difference in the electron density, which has also been reflected by the H_2O_2 concentrations obtained in PAW, namely higher concentration in the Ar discharge treated water. The emission intensity of the NOγ bands are also stronger in the argon discharge, however, due to the strong quenching of the excited NO molecules by N_2, this emission can indicate well the presence of NO molecules. In the present work the possibilities given by the nitrogen jet are investigated in detail.

First of all, the evolution of the PAW composition with the treatment time in different treated volumes is investigated. Figure 8 shows the concentrations of the nitrate, nitrite, hydrogen peroxide, as well as the pH as a function of treatment time in the case of 25, 125 and 200 ml treated water. The concentrations have been measured at every six minutes during the treatment. It is found that during the treatment the H_2O_2 concentration increases linearly independently of the treated volume. On the other hand, the and NO_3^- and NO_2^- concentrations show a saturation at the lower 25 ml treated volume, which can be related to the recombination processes involving H_2O_2, that is produced here in higher concentration. This effect does not appear at the higher treated volumes, thanks to the lower H_2O_2 concentrations obtained during the same treatment time. The pH is found to decrease linearly with the treatment time, which is related to the increase of the nitrite and nitrate concentrations. The error bars shown in

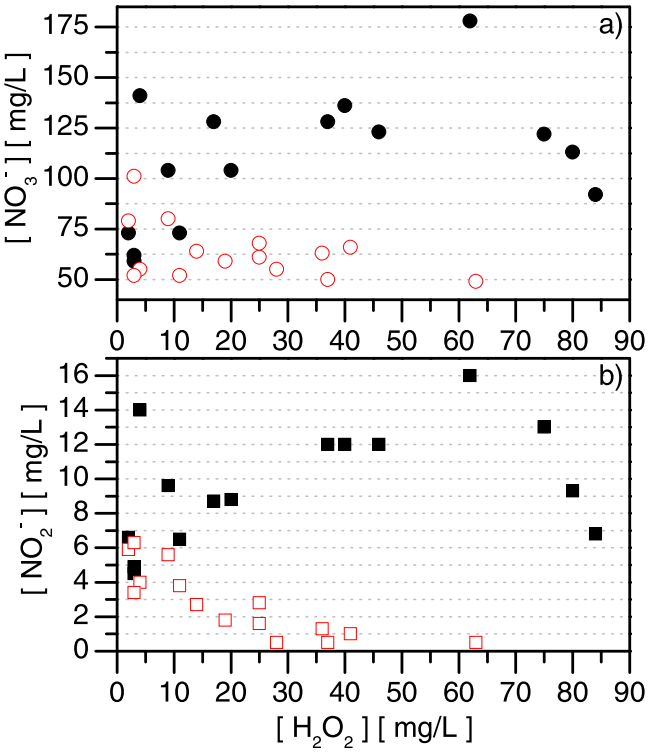

Figure 5. The nitrate-hydrogen peroxide (a) and nitrite-hydrogen peroxide concentration (b) maps right after the plasma treatment (closed symbols) and one hour storage (open symbols). The data correspond to all the conditions listed in table 2.

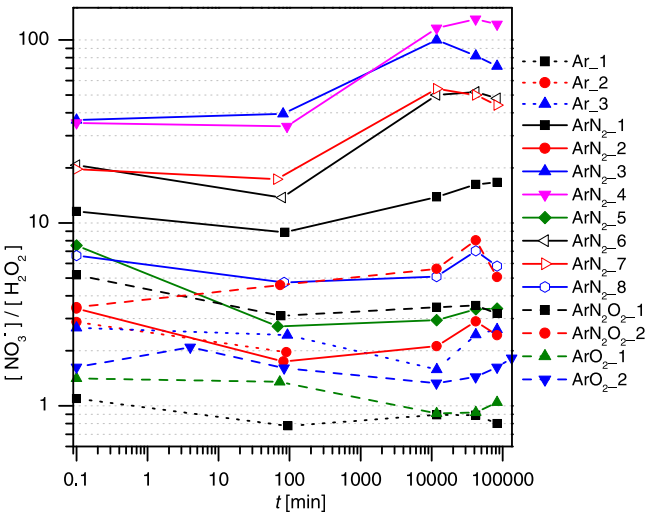

Figure 6. The ratio of the nitrate to peroxide concentration as a function of ageing time for the different treatment conditions as listed in table 2.

figure are obtained by averaging four independent sample treatments. The treatment of the smallest volume is the most sensitive case, the errors are due to the adjustment of the capillary orifice—water surface distance, which can slightly change also during treatment due to the water evaporation.

Figure 9 shows the evolution of the concentrations and pH during the storage at room temperature of PAWs produced in different volumes. Similarly to the PAW produced by the surface-wave microwave discharge, the post-discharge

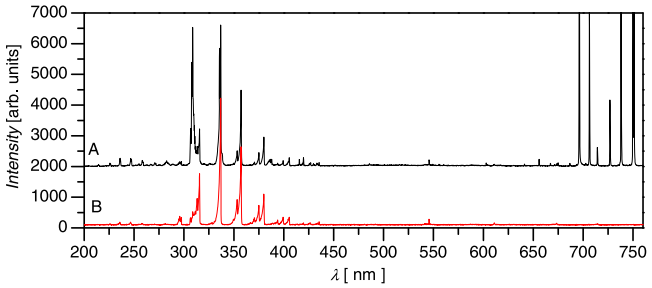

Figure 7. The optical emission spectra of the argon (A) and nitrogen (B) kHz plasma jets recorder from the region right below the capillary exit.

evolution of radicals in PAW strongly depends on the absolute concentrations. Accordingly, the sharpest first phase decrease can be observed in the smallest 25 ml volume PAW, where the highest concentrations have been obtained. Especially, the NO_2^- concentration drops fast, due to the recombination of NO_2^- with H_2O_2. In the larger, less concentrated volume, with the lowest initial H_2O_2 concentration, the nitrite and nitrate recombination is more moderate, with the NO_2^- being preserved for months.

In the case of the nitrogen kHz plasma jet one controlling parameter can be the treatment distance. Figure 10 shows the concentrations obtained by treating the 25 ml volume at different capillary orifice to the water surface distances. As expected, with the decrease of the distance, due to the increase of the electron density the formation of H_2O_2 radicals is strongly enhanced, while the nitrate and nitrite concentrations change just slightly. Accordingly, with this method the $[NO_3^-]/[H_2O_2]$ concentration ratio could be varied in the 2–12 range. However the ageing tends to equalize this ratio.

3.3. Controlling the ageing of PAW

As we have seen, the most affected radical by storage is the NO_2^-, and its evolution strongly depends on the H_2O_2 concentration. In order to preserve the NO_2^-, the concentration of H_2O_2 and its recombination should be controlled. One possibility is to rely on a Fenton type reaction, which controls the H_2O_2 recombination. This reaction is believed to have more pathways: (i) the Fenton $M^{2+} + H_2O_2 \rightarrow M^{3+} + OH + OH^-$ or (ii) the catalase $M^{2+} + H_2O_2 \rightarrow MO^{2+} + H_2O$, $MO^{2+} + H_2O_2 \rightarrow M^{2+} + H_2O + O_2$. In our study we use copper as a metal.

In order to test this effect, we compared the evolution of two different samples produced under same treatment conditions: (i) plasma-activated water (PAW) and (ii) plasma-activated water with a copper plate inserted during the treatment (PAW+Cu). The applied copper plate is 1 mm thick of 70×10 mm^2 size. Figure 11 shows the ageing of the samples activated with the surface-wave microwave discharge. The results illustrate, that copper contributes to the increase of the H_2O_2 recombination, while it slows down that of the NO_2^-. In this way NO_2^- can be preserved longer (We note that the effect depends on the concentration of H_2O_2.). This indicates that the copper mediated H_2O_2 recombination changes the system's chemical kinetics. In order to be able to control the ageing of PAW, a deeper understanding of the

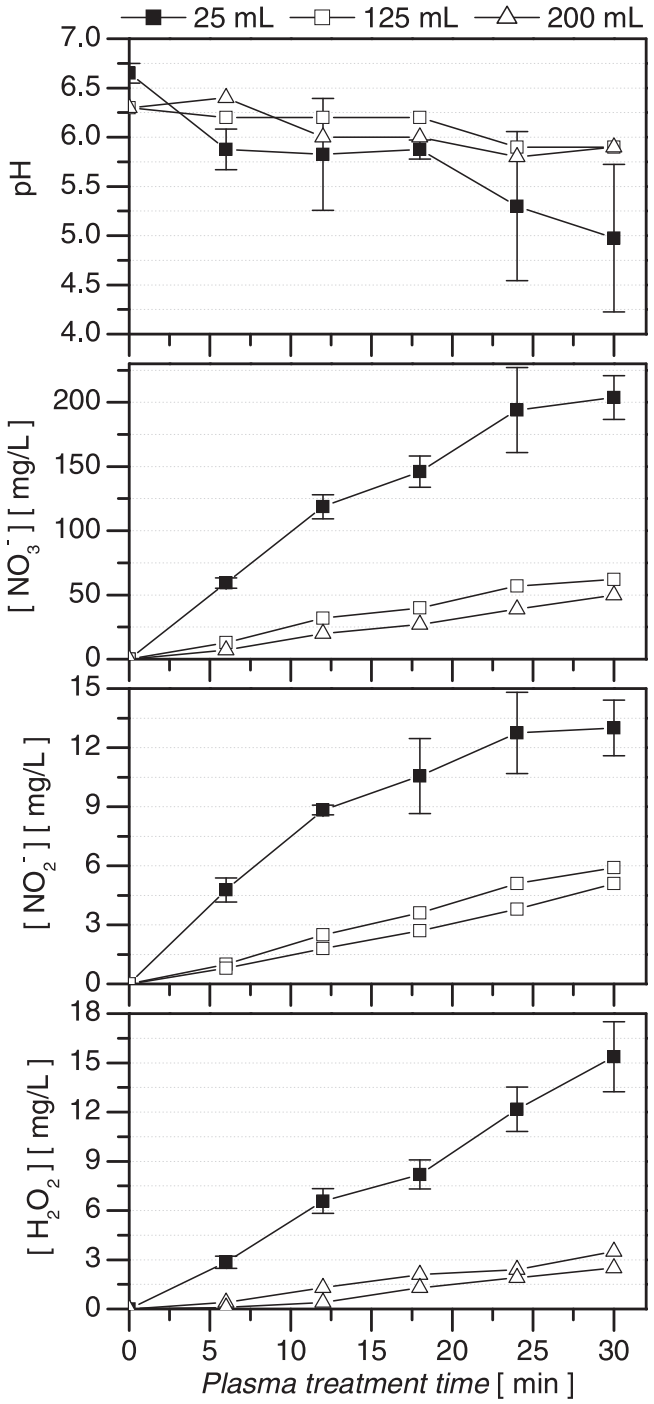

Figure 8. The evolution of the concentrations and the pH during 30 min treatment with the nitrogen atmospheric pressure plasma jet in the case of different treated volumes. The discharge is sustained with 12 kV and 28 kHz sinusoidal waveform, and the capillary-water surface distance is 10 mm.

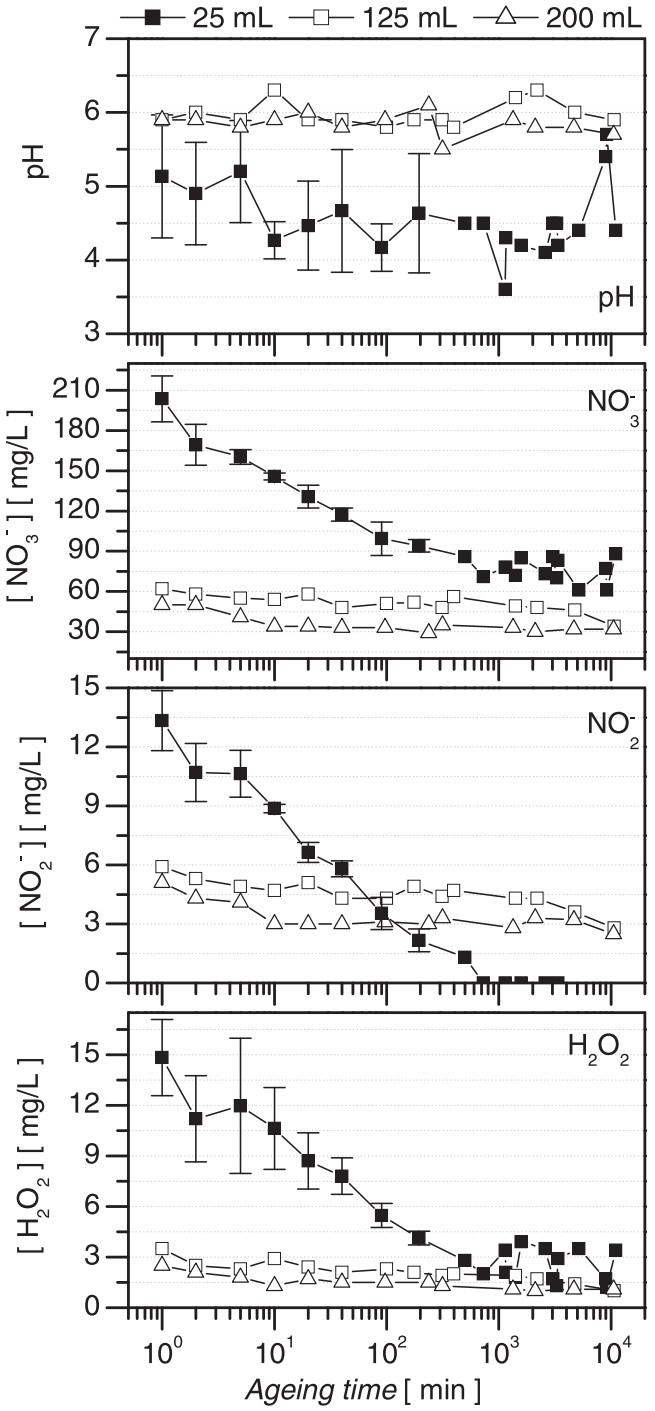

Figure 9. Ageing at room temperature of PAWs obtained by 30 min nitrogen plasma jet treatment.

chemical pathways is required, which can be the focus of a future work.

4. Summary

An atmospheric pressure surface-wave microwave discharge and a kHz plasma jet have been used to activate purified water (W) and to study the possibility to tune the composition of plasma activated water (PAW) with the discharge and treatment conditions.

The surface-wave microwave discharge has been ignited in Ar and in $Ar/N_2/O_2$ binary and ternary mixtures with powers in the 25–30 W range. The different gas mixture conditions allows to tune the electron and species densities at the plasma-water interaction point. The treatments have been conducted by putting 32 ml W in contact with the plasma plume, with the water surface being at 5.5, 8.5 and 10.5 mm

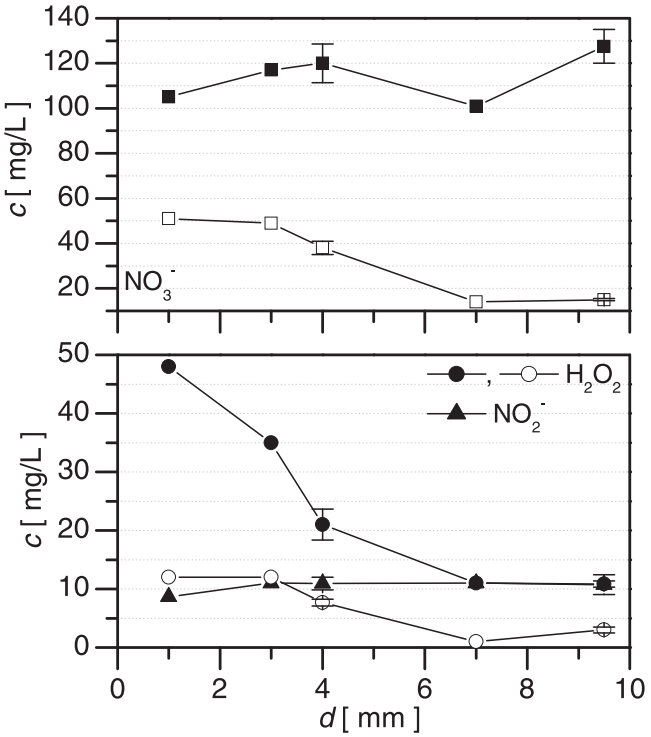

Figure 10. Concentrations as a function of treatment distance within the first minute after treatment (full symbols) and after 50 000 min (35 d) storage (open symbols) in the case of 25 ml 10 min plasma jet treatment.

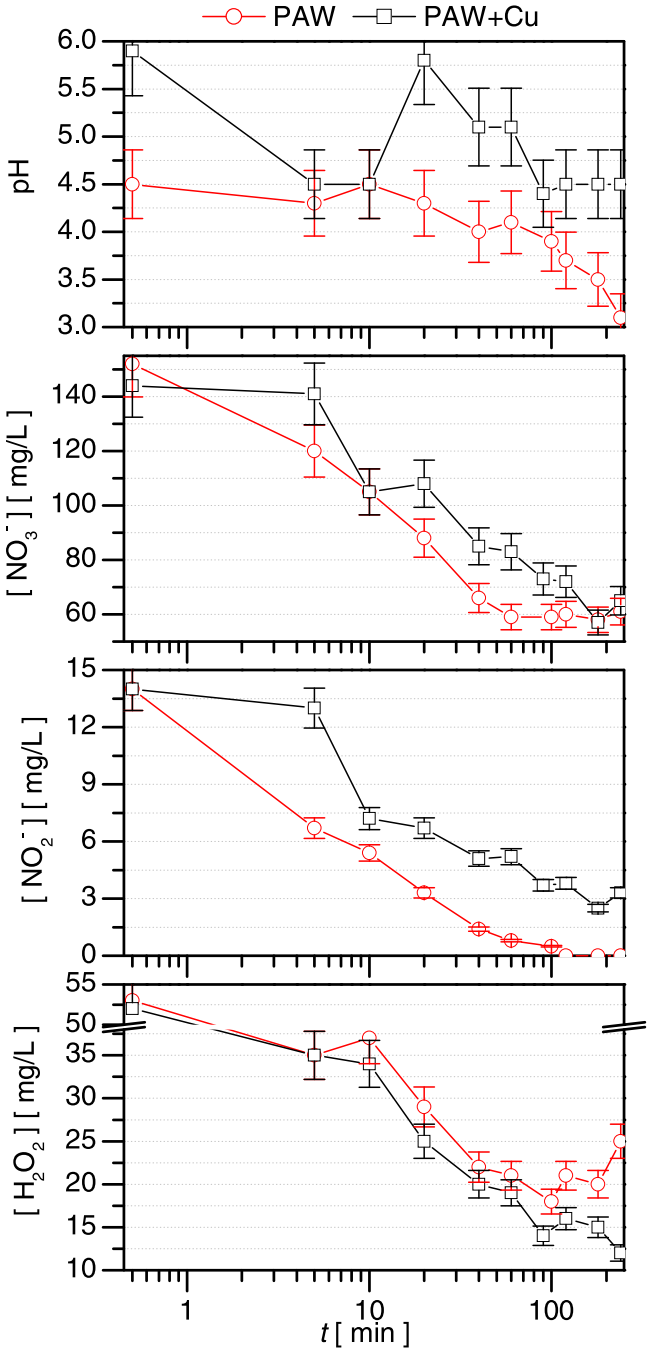

Figure 11. Ageing of microwave produced PAWs: plasma-activated water (PAW) and plasma-activated water with a copper plate inserted during the treatment (PAW+Cu).

distances from the edge of the discharge quartz tube. It is shown, that by varying the initial gas mixture composition and treatment distance, the absolute radical concentrations in the plasma activated water (PAW) can be varied in the range of 0.5–85 mg l^{-1} for H_2O_2, 20–180 mg l^{-1} for NO_3^- and 0.5–14 mg l^{-1} for NO_2^-. The ageing of PAW is found to depend on the absolute concentration of radicals, and most specifically on the concentration of H_2O_2, which governs first of all the recombination of NO_2^-. When the initial concentrations of H_2O_2 and NO_3^- are higher than about 60 mg l^{-1}, a sharp decrease of both concentrations occurs within the first hour, while the NO_2^- radicals recombine totally. At lower initial H_2O_2 concentrations (10–40 mg l^{-1}), the recombination rates for both H_2O_2 and NO_3^- become smaller, more pronouncedly in the case of H_2O_2. Finally, when the initial H_2O_2 concentration is lower than 5 mg l^{-1} the H_2O_2 radicals disappear totally within one week, while the NO_2^- can survive more than one month. It is further found, that the concentration ratio of NO_3^- and H_2O_2 radicals is varied over three orders of magnitude, which is preserved during months of storage at room temperature. The pH of PAWs right after the treatment have values between 5 and 6, and a correlation is found between the pH and the nitrite/nitrate concentrations, namely, at higher nitrate concentration lower pH is obtained. During the first hour of ageing, in the PAWs where a sharp decrease of the concentrations occurred —which exclude conditions where the H_2O_2 concentration is initially very low—, the pH decreased to values between 4.4 and 5.5. However, at the latter stage of ageing, with the stabilization of the concentrations the pH increased again to values between 5.8 and 6.7. A correlation is found between the pH variation and the H_2O_2 recombination.

The kHz plasma jet has been ignited in N_2 gas with a sinusoidal voltage waveform of 28 kHz and maximum voltage of 12 kV. With this source the effect of the treatment distance and treated volume on the PAW composition has been studied. It is shown, that by varying the distance in the 1–10 mm range, the $[NO_3^-]/[H_2O_2]$ concentration ratio can be tuned within one order of magnitude, which is partially preserved during ageing. At the same time, the absolute concentrations in the 25 ml

PAW vary in the 0.5–50 mg l^{-1} for H_2O_2, 15–130 mg l^{-1} for NO_3^- and 0.5–10 mg l^{-1} for NO_2^-. With the increase of the treated volume up to 200 ml, lower radical concentrations are achieved, with the H_2O_2 reaching as low as 4 mg l^{-1}, which results in the fast recombination of H_2O_2 and the preservation of NO_2^- for months.

In order to control the H_2O_2 concentration and thus the NO_2^- radicals recombination, the application of a Fenton type reaction is suggested, where the H_2O_2 recombination is mediated by metal ions. By inserting a copper surface into PAW during or after plasma treatment, it is demonstrated that the recombination pathway of H_2O_2 can be altered, and the NO_2^- radicals can be preserved longer.

Acknowledgments

The work has been supported by the Hungarian Science Foundation NKFIH, through project K-115805, by the Croatian Science Foundation, through project IP-2013-11-2753 and by the Croatian—Hungarian bilateral project TéT_16-1-2016-0014.

ORCID iDs

Kinga Kutasi https://orcid.org/0000-0001-6082-1853
Dean Popović https://orcid.org/0000-0003-3906-3482
Nikša Krstulović https://orcid.org/0000-0001-6443-2417
Slobodan Milošević https://orcid.org/0000-0002-4455-7869

References

[1] Kamgang-Youbi G, Herry J-M, Bellon-Fontaine M-N, Brisset J-L, Doubla A and Naïtali M 2007 *Appl. Environ. Microbiol.* **73** 4791
[2] Kamgang-Youbi G, Herry J-M, Brisset J-L, Bellon-Fontaine M-N, Doubla A and Naïtali M 2008 *Appl. Microbiol. Biotechnol.* **81** 449
[3] Naïtali M, Kamgang-Youbi G, Herry J-M, Bellon-Fontaine M-N and Brisset J-L 2010 *Appl. Environ. Microbiol.* **76** 7662
[4] Ikawa S, Kitano K and Hamaguchi S 2010 *Plasma Process. Polym.* **7** 33
[5] Traylor M J, Pavlovich M J, Karim S, Hait P, Sakiyama Y, Clark D S and Graves D B 2011 *J. Phys. D: Appl. Phys.* **44** 472001
[6] Oehmigen K, Hähnel M, Brandenburg R, Wilke C, Weltmann K-D and von Woedtke T 2010 *Plasma Process. Polym.* **7** 250
[7] Oehmigen K, Winter J, Hähnel M, Wilke C, Brandenburg R, Weltmann K-D and von Woedtke T 2011 *Plasma Process. Polym.* **8** 904
[8] Kobayashi T, Iwata N, Oh J-S, Hashizume H, Ohta T, Takeda K, Ishikawa K, Hori M and Ito M 2017 *J. Phys. D: Appl. Phys.* **50** 155208
[9] Tasaki T, Ohshima T, Usui E, Ikawa S, Kitano K, Maeda N and Momoi Y 2017 *Dent. Mater. J.* **36** 422
[10] Tanaka H, Mizuno M, Ishikawa K, Nakamura K, Kajiyama H, Kano H, Kikkawa F and Hori M 2011 *Plasma Med.* **1** 265
[11] Utsumi F, Kajiyama H, Nakamura K, Tanaka H, Mizuno M, Ishikawa K, Kondo H, Kano H, Hori M and Kikkawa F 2013 *PLoS One* **8** e81576
[12] Takai E, Ohashi G, Yoshida T, Särgjerd K M, Zako T, Maeda M, Kitano K and Shiraki K 2014 *Appl. Phys. Lett.* **104** 023701
[13] Puač N, Gherardi M and Shiratani M 2017 *Plasma Process. Polym.* **15** 1700174
[14] Sivachandiran L and Khacef A 2017 *RSC Adv.* **7** 1822
[15] Thirumdas R, Kothakota A, Annapure U, Siliveru K, Blundell R, Gatt R and Valdramidis V P 2018 *Trends Food Sci. Technol.* **77** 21?31
[16] Jukák J, Scholtz V, Kotúčová S and Janoušková O 2012 *Phys. Med.* **28** 230
[17] Brisset J-L and Pawlat J 2016 *Plasma Chem. Plasma Process.* **36** 355
[18] Laurita R, Barbieri D, Gherardi M, Colombo V and Lukes P 2015 *Clin. Plasma Med.* **3** 53
[19] Shen J, Tian Y, Li Y, Ma R, Zhang Q, Zhang J and Fang J 2016 *Sci. Rep.* **6** 28505
[20] Julák J, Hujacová A, Scholtz V, Khun J and Holada K 2018 *Plasma Phys. Rep.* **44** 125
[21] Lukes P, Dolezalova E, Sisrova I and Clupek M 2014 *Plasma Sources Sci. Technol.* **23** 015019
[22] Ito T, Uchida G, Nakajima A, Takenaka K and Setsuhara Y 2017 *Japan. J. Appl. Phys.* **56** 01AC06
[23] Wang B, Liu D, Zhang Z, Li Q, Liu Z, Guo L, Wang X and Kong M G 2017 *J. Phys. D: Appl. Phys.* **50** 305202
[24] Zaplotnik R, Kregar Z, Bišćan M, Vesel A, Cvelbar U, Mozetič M and Milošević S 2014 *Eur. Phys. Lett.* **106** 25001
[25] Machala Z, Tarabova B, Hensel K, Spetlikova E, Sikurova L and Lukes P 2013 *Plasma Process. Polym.* **10** 649
[26] Krcma F, Tsonev I, Smejkalová K, Truchlá D, Kozáková Z, Zhekova M, Marinova P, Bogdanov T and Benova E 2018 *J. Phys. D: Appl. Phys.* **51** 414001
[27] Kutasi K, Noel C, Belmonte T and Guerra V 2016 *Plasma Sources Sci. Technol.* **25** 055014
[28] Moisan M and Zakrzewski Z 1991 *J. Phys. D: Appl. Phys.* **24** 1025
[29] Kutasi K, Sá P and Guerra V 2012 *J. Phys. D: Appl. Phys.* **45** 195205
[30] Brisset J-L and Hnatiuc E 2012 *Plasma Chem. Plasma Process.* **32** 655
[31] Lobachev V L and Rudakov E S 2006 *Russ. Chem. Rev.* **75** 375
[32] Liu F *et al* 2010 *Plasma Process. Polym.* **7** 231
[33] Pavlovich M J, Chang H-W, Sakiyama Y, Clark D S and Grave D B 2013 *J. Phys. D: Appl. Phys.* **46** 145202
[34] Ercan U K, Wang H, Ji H, Fridman G, Brooks A D and Joshi S G 2013 *Plasma Process. Polym.* **10** 544
[35] van Gils C A J, Hofmann S, Boekema B K H L, Brandenburg R and Bruggeman P J 2013 *J. Phys. D: Appl. Phys.* **46** 175203
[36] Girard F, Badets V, Blanc S, Gazeli K, Marlin L, Authier L, Svarnas P, Sojic N, Clément F and Arbault S 2016 *RSC Adv.* **6** 78457
[37] Vlad I-E and Anghel S D 2017 *J. Electrostat.* **87** 284
[38] Chen Z, Liu D, Chen C, Xu D, Liu Z, Xia W, Rong M and Kong M G 2018 *J. Phys. D: Appl. Phys.* **51** 325201
[39] Oh J-S, Szili J E, Ogawa K, Short R D, Ito M, Furuta H and Hatta A 2018 *Japan. J. Appl. Phys.* **57** 0102B9